Controlling a Quadcopter with Static Loads and Dynamic Wind Disturbances using a Fuzzy Controller

Aida Azka
Department of Electrical Engineering
Institut Teknologi Sepuluh Nopember
Surabaya, Indonesia
azkaaida9@gmail.com

Ari Santoso
Department of Electrical Engineering
Institut Teknologi Sepuluh Nopember
Surabaya, Indonesia
santoso@ee.its.ac.id

Trihastuti Agustinah
Department of Electrical Engineering
Institut Teknologi Sepuluh Nopember
Surabaya, Indonesia
trihastuti@its.ac.id

***Abstract*— Maneuverability, hover, and simple mechanical design are the advantages of quadcopters. However, because quadcopters are smaller and lighter, they are more susceptible to wind than manned aircraft. The winds that cause air accidents are divided into several categories, namely downburst, turbulent wind, wind shear, and wind vortices. Disturbances and uncertainties, such as wind gusts, can result in difficulties in executing a mission on an accurate flight path. Quadcopter resilience is an important topic for UAV (unmanned aerial vehicle). Especially if the quadcopter is in terrain that is difficult for humans to reach. Hence, the system is susceptible and experiences reduced stability. Controlling a quadcopter with a cube-shaped static load to withstand turbulent wind gusts in this research uses a Fuzzy controller with LQR (Linear Quadratic Regulator) output feedback and an LQR output feedback controller with CGT (Command-Generator Tracking). The results achieved through fuzzy control can protect the quadcopter against half of the overall turbulent wind gusts with an RMSE (Root Mean Square Error) from the x, y and z axes of 0.0183; 0.0212; and 0.0822. In contrast to the LQR-CGT control which still shows an RMSE from the x, y and z axes of 0.0755; 0.0516; 0.0848.**

Keywords*— fuzzy, load, quadcopter, wind turbulence.

I. INTRODUCTION

Interest in studying UAVs throughout the country is very large, one of which is multirotor UAVs such as quadcopters which are also in research [1], [2], [3]. In [4] explains that maneuverability, hover, and simple mechanical design are the advantages of quadcopters. As technology develops, quadcopters are widely used to help make human work easier without a crew on board. According to [5], Quadcopters are often used in the fields of surveillance and mapping, search and rescue missions, liquid spraying, logistics delivery, as well as military and security applications.

Research [6] states that quadcopters, being smaller and lighter, are more susceptible wind compared with manned aircraft. It was also explained that the winds that cause air accidents are divided into several categories, namely downburst, turbulent wind, wind shear and wind vortices. Disturbances and uncertainties such as wind gusts can result in difficulties in executing a mission on an accurate flight path. The resilience of quadcopters is a crucial aspect for UAVs when dealing with external disturbances beyond human control. This is particularly important when the quadcopter operates in terrains that are difficult for humans to reach, such as mountain peaks, open seas, or other extreme environments. In such conditions, the system is easily affected and may become less stable.

In this research we will discuss the resistance of a quadcopter carrying a cube-shaped load to wind turbulence which has not been discussed in research [6]. The quadcopter used in this research is the Qball X4 with a wind model in the form of a Dryden turbulent wind model where in research [1] does not yet have a specific wind model. To keep the quadcopter on its trajectory, the author applies a Linear Quadratic Regulator (LQR) output feedback controller with a Command Generator Tracker (CGT) as in research [1], [2], which has succeeded in controlling the position of the UAV. To maintain the stability of the quadcopter when wind turbulence occurs, the author will try to use a fuzzy controller to control the quadcopter's position with LQR feedback output to control the quadcopter's attitude. As stated in research [7], fuzzy aims to increase the stability of the quadcopter in the presence of disturbances. However, if a quadcopter flies through wind turbulence, this has not been discussed in research [7]. From there, the UAV's resistance to turbulent wind disturbances was developed in this research. The expected contribution of this research is that it can help reduce air accidents caused by quadcopters that cannot complete their missions while carrying a payload because they are thrown off course when wind turbulence occurs in the wild, which previous researchers have not widely discussed.

II. METHODS

A. Quadcopter Model

The quadcopter dynamics model can be represented from the following transformation matrix. The dynamics of translational motion in a quadcopter is based on Newton's second law:

$$\Sigma F = ma \tag{1}$$

$$F_f + F_g = m\ddot{\xi} \tag{2}$$

where

$$\xi = [x \quad y \quad z]^T \tag{3}$$

$$F_f = [F_x \quad F_y \quad F_z]^T \tag{4}$$

$$F_g = [0 \quad 0 \quad -mg]^T \tag{5}$$

Quadcopter modeling regarding the working axis can be represented in the body frame and earth frame transformation matrix equations found in [3].

$$R_B = R_{zyx}(\phi,\theta,\psi) = R_z(\psi).R_y(\theta).R_x(\phi)$$

$$= \begin{bmatrix} c\theta c\psi & s\phi s\theta c\psi - c\phi s\psi & c\phi s\theta c\psi + s\phi s\psi \\ c\theta s\psi & s\phi s\theta s\psi + c\phi c\psi & c\phi s\theta s\psi - s\phi c\psi \\ -s\theta & s\phi c\theta & c\phi c\theta \end{bmatrix} \tag{6}$$

where $c\phi = \cos\phi$, $c\theta = \cos\theta$, $c\psi = \cos\psi$, $s\phi = \sin\phi$, $s\theta = \sin\theta$, and $s\psi = \sin\psi$.

How to cite: Azka, A., Santoso,A., Agustinah, T. (2024). Controlling a Quadcopter with Static Loads and Dynamic Wind Disturbances using a Fuzzy Controller. *JAREE (Journal on Advanced Research in Electrical Engineering), 8(2).*

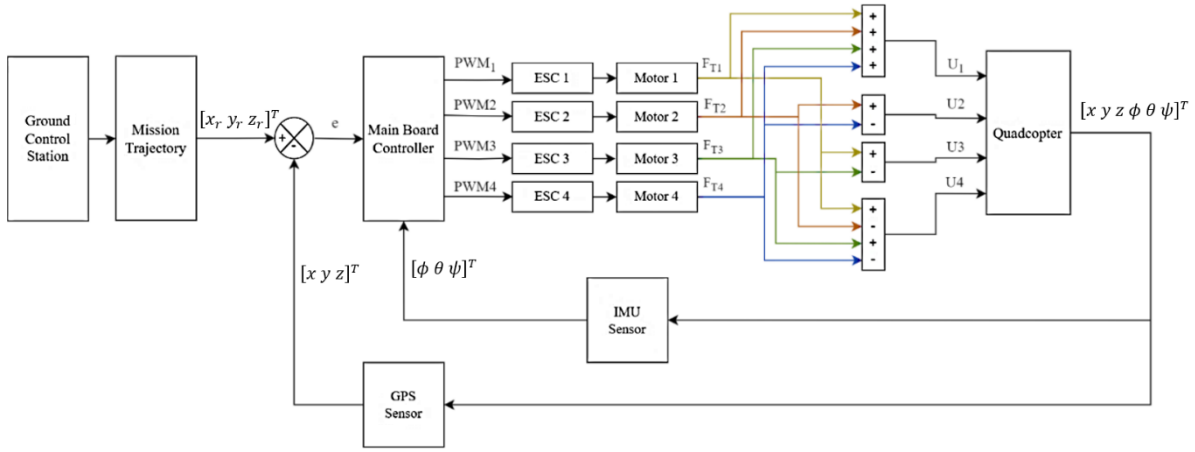

Fig. 1. Block diagram of quadcopter design

TABLE 1. QUADCOPTER PARAMETERS [1].

Parameters	Symbol	Value
Mass Quadcopter	m_Q	1.4 kg
Mass Battery	m_B	0.4 kg
Mass Load	m_L	1.699 kg
Gravity	g	9.81 kg/m^2
Load surface area	A	0.06 m^2
Arm length	l	0.2 m
Inertia Moment (x)	I_{xx}	0.03 kg.m^2
Inertia Moment (y)	I_{yy}	0.03 kg.m^2
Inertia Moment (z)	I_{zz}	0.04 kg.m^2
Actuator bandwidth	ω	15 rad/s
Constant thrust force	K	120 N

The force acting on the quadcopter is generated by the four motors with their propellers. The impact of quadcopter's aerodynamic forces is minimal, thus it can be disregarded in modeling [1].

$$U_1 = F_{T_1} + F_{T_2} + F_{T_3} + F_{T_4} \quad (7)$$

$$U_2 = l(F_{T_2} - F_{T_4}) \quad (8)$$

$$U_3 = l(F_{T_1} - F_{T_3}) \quad (9)$$

$$U_4 = d(F_{T_1} + F_{T_2} + F_{T_3} + F_{T_4}) \quad (10)$$

where d is the drag force constant, F_{T_i} is the list produced by each motor propeller (see in Fig. 1) which is defined in [2] as:

$$F_{T_i} = K\frac{\omega}{s+\omega}u_i \quad (11)$$

where K is the trusht constant, ω is the motor bandwidth, and u_i is the control signal for each motor.

The load attached to the quadcopter body can be written using the equation from [6], [8]:

$$F_L = \frac{1}{M_t}\begin{bmatrix} A_x & 0 & 0 \\ 0 & A_y & 0 \\ 0 & 0 & A_z \end{bmatrix}\begin{bmatrix} \dot{x} \\ \dot{y} \\ \dot{z} \end{bmatrix} \quad (12)$$

where F_L is the force that occurs when the wind collides with a load, M_t is total mass, and A_i is surface area of cube.

B. *Dryden Wind Noise Model*

Wind speed is a prerequisite for dynamic modelling of UAVs while in the field. In certain areas, [9] applies the wind that is felt or appears at certain times is wind turbulence. The turbulent wind speed model is obtained from the Dryden model with a special transfer function and simulates real turbulent winds based on [9].

In the Dryden model, [10] explains that there are three white noises each representing $\Phi_u(\omega)$, $\Phi_v(\omega)$, $\Phi_w(\omega)$ and $\Phi_p(\omega)$, $\Phi_q(\omega)$, $\Phi_r(\omega)$ which are defined by velocity and angular rate. These three noises are components of different turbulence directions that follow a Gaussian distribution. The spectra functions of longitudinal, lateral, and vertical are explained in [11] as follows.

1) Longitudinal

$$\Phi_u(\omega) = \frac{2\sigma_u^2 L_u}{\pi V}\cdot\frac{1}{1+\left(L_u\frac{\omega}{V}\right)^2} \quad (13)$$

$$\Phi_p(\omega) = \frac{\sigma_w^2}{VL_w}\cdot\frac{0.8\left(\frac{2\pi L_w}{4b}\right)^{\frac{1}{3}}}{1+\left(\frac{4b\omega}{\pi V}\right)^2} \quad (14)$$

2) Lateral

$$\Phi_v(\omega) = \frac{2\sigma_v^2 L_v}{\pi V}\cdot\frac{1+12\left(L_v\frac{\omega}{V}\right)^2}{\left[1+4\left(L_v\frac{\omega}{V}\right)^2\right]^2} \quad (15)$$

$$\Phi_q(\omega) = \frac{\pm\left(\frac{\omega}{V}\right)^2}{1+\left(\frac{4b\omega}{\pi V}\right)^2}\cdot\Phi_w(\omega) \quad (16)$$

3) Vertical

$$\Phi_w(\omega) = \frac{2\sigma_w^2 L_w}{\pi V}\cdot\frac{1+12\left(L_w\frac{\omega}{V}\right)^2}{\left[1+4\left(L_w\frac{\omega}{V}\right)^2\right]^2} \quad (17)$$

$$\Phi_r(\omega) = \frac{\pm\left(\frac{\omega}{V}\right)^2}{1+\left(\frac{3b\omega}{\pi V}\right)^2}\cdot\Phi_v(\omega) \quad (18)$$

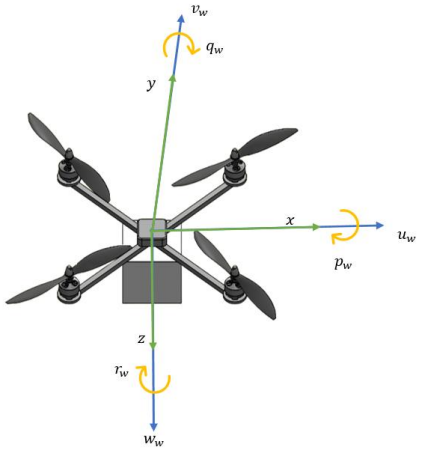

Fig. 2. Definition of the linear speed and the angular speed axis of the turbulent wind based on the quadcopter body axis [11]

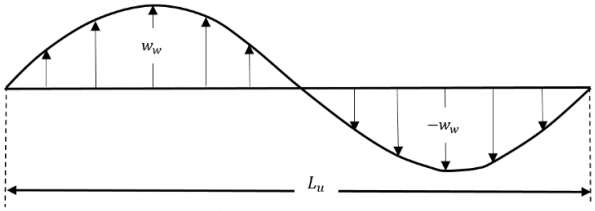

Fig. 3. Illustration of the quadcopter flies into a sine-type turbulence field [11]

Equation (13) until (18), it can be seen that σ_u, σ_v, and σ_w are turbulence intensities which describe the magnitude of wind speed fluctuations respectively in the longitudinal, lateral, and vertical directions such as the quadcopter body axis in Fig. 2. The turbulence scale lengths are L_u, L_v, and L_w that indicate the characteristic size of the wind vortices in these three directions which can be seen in Fig. 3. Meanwhile, b is the wingspan of the aircraft which is used as a reference in calculating the effects of turbulence on the aircraft. However, other relevant parameters instead of wingspan were used in this study because quadcopters do not have wings like airplanes. The replacement parameter for wing span is using the diagonal of the quadcopter. This diagonal is the total length of the system including the height from the highest point of the quadcopter to the lowest point of the load cube because it represents the main dimensions that influence the aerodynamic response of the quadcopter to turbulence. For a quadcopter flying at speed V (see in Fig. 4) through a frozen turbulence field with a spatial frequency of Ω radians per meter, the circular frequency ω is calculated by multiplying V by Ω. In this context, frozen turbulence means that the turbulence pattern is considered stationary and does not change over time. The spatial frequency Ω represents the rate of spatial variation in turbulence, indicating how quickly the turbulence changes with distance. The circular frequency ω, given by the formula $\omega = V \cdot \Omega$, reflects the rate at which the quadcopter experiences these variations in turbulence over time. These relationships are important for understanding the dynamic response of quadcopters to turbulent conditions and for modeling and predicting the impact of turbulence on quadcopter stability and control.

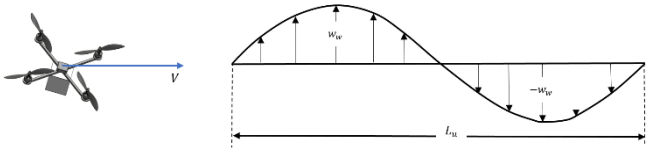

Fig. 4. Illustration of a quadcopter entering a sine-type turbulence field [11]

C. *LQR* with *Command-Generator Tracker*

The quadcopter control in [1], [2] is used to keep the quadcopter following the reference trajectory, namely by using LQR output feedback with the Command Generator Tracker. The error of the quadcopter trajectory is obtained from calculating the difference between the actual feedback output state z, ϕ, θ, ψ and the reference input state z_d, ϕ_d, θ_d, ψ_d by using gain performance output feedback, an integrator on the feedforward compensator, and modifying the input control to provide zero steady-state error [12]. So that the tracking error does not have a large value, an integrator is added to the control structure, and the model system is written as:

$$\dot{x} = Ax + Bu$$
$$y = Cx \tag{19}$$

where state $(t) \in R^n$, control input $u(t) \in R^m$, and measurement output $y(t) \in R^p$.

The objective of implementing LQR output feedback for the system is driving errors to zero, ensuring stability is upheld. The controller performance index can be seen in [12] as follows:

$$J = \frac{1}{2}\int_0^\infty (x^T Q x + u^T R u)dt \tag{20}$$

where Q and R are positive semidefinite symmetric weighting matrices. Therefore, assuming certainty regarding Q and R ensures that J is not negative and results in a minimization problem.

In CGT, assume the reference signal $r(t)$ is as follows:

$$r^{(d)} + a_1 r^{(d-1)} + \cdots + a_d r = 0 \tag{21}$$

If d and a_i have certain values, then the canonical form of observability of the equation is obtained:

$$\dot{\rho} = \begin{bmatrix} 0 & 1 \\ -a_2 & -a_1 \end{bmatrix} \rho \equiv G\rho \tag{22}$$

In bandwidth actuator dynamics, a reference signal is required to obtain CGT control. However, the derivative of the reference signal is not fully used as a design specification for a proper CGT. Thus, the conversion transcription target becomes a regulatory target where the resulting error must approach zero over an infinite time horizon ($t \to \infty$) with the formula:

$$\Delta(s)e = \Delta(s)r - \Delta(s)Hx = -H\xi$$
$$\dot{\varepsilon} = G\varepsilon + \begin{bmatrix} 0 \\ -H \end{bmatrix} \xi \tag{23}$$

where

$$\xi = \Delta(s)x = x^d + a_1 x^{d-1} + \cdots + a_d x \tag{24}$$

Based on (23) and (28) we get:

$$\dot{\xi} = A\xi + B\tilde{u} \tag{25}$$

with the control input adjusted as:

$$\tilde{u} = \Delta(s)u = u^{(d)} + a_1 u^{(d-1)} + \cdots + a_d u \quad (26)$$

Then the modified system equation becomes:

$$\dot{\tilde{x}} = \tilde{A}\tilde{x} + \tilde{B}\tilde{u}$$

$$\frac{d}{dt}\begin{bmatrix}\varepsilon \\ \xi\end{bmatrix} = \begin{bmatrix} G & \vdots & 0 \\ \cdots & \vdots & -H \\ 0 & \vdots & A \end{bmatrix}\begin{bmatrix}\varepsilon \\ \xi\end{bmatrix} + \begin{bmatrix}0 \\ B\end{bmatrix}\tilde{u} \quad (27)$$

If the system state becomes zero, then there is no encryption error. This is because the LQR design is implemented in the new system. The results of the control input modification are written as:

$$\tilde{u} = -[K_\varepsilon \quad K_y]\begin{bmatrix}\varepsilon \\ C\xi\end{bmatrix} = -\tilde{K}\tilde{y} \quad (28)$$

The control law in (31) is solved by LQR output feedback. Therefore, the output feedback equation for LQR is:

$$\frac{\partial H}{\partial S} = \tilde{A}_c^T P + P\tilde{A}_c + \tilde{C}^T\tilde{K}^T R\tilde{K}\tilde{C} + Q = 0 \quad (29)$$

$$\frac{\partial H}{\partial P} = \tilde{A}_c S + S\tilde{A}_c^T + E_X = 0 \quad (30)$$

$$\frac{1}{2}\frac{\partial H}{\partial K} = R\tilde{K}\tilde{C}S\tilde{C}^T - \tilde{B}^T P S\tilde{C}^T = 0 \quad (31)$$

where $\tilde{A}_c = \tilde{A} - \tilde{B}\tilde{K}\tilde{C}$ dand $E_X = E\{Ex(0)x^T(0)\}$

If the conditions for the weighting matrix $R > 0$ and $\tilde{C}S\tilde{C}^T$ are met, then the output feedback gain $\tilde{K}$ is formed as:

$$\tilde{K} = \mathrm{R}^{-1}\tilde{B}^{\mathrm{T}}\mathrm{PS}\tilde{C}^{\mathrm{T}}\left(\tilde{C}\mathrm{S}\tilde{C}^{\mathrm{T}}\right)^{-1} \quad (32)$$

D. Fuzzy Controller

The fuzzy controller used in this study aims to regulate the quadcopter's trajectory, minimizing errors in the presence of wind turbulence. One of the intelligent control systems that has been widely used is fuzzy. In research [13], the benefits of fuzzy logic controllers over traditional controllers are described, including straightforward control, cost-effectiveness, and the ability to design them without needing the mathematical model of the process beforehand. Fuzzy logic was created to address the concept of values that fall between true and false. Using fuzzy logic, the resulting values are not limited to 1 and 0, but encompass all possibilities between 0 and 1.

Linear representation, the mapping of input onto its membership degrees is depicted as a straight line. In this representation, there are two states of the fuzzy set, namely an increase which has a membership degree of zero leading to a higher one and a second state, namely a decrease which is the opposite of the increasing linear representation. The ascending linear representation membership function can be seen in [13], [14] as follows:

$$\mu[x] = \begin{cases} 0; & x \le a \\ \dfrac{x-a}{b-a}; & a \le x \le b \\ 1; & x \ge b \end{cases} \quad (33)$$

The descending linear representation membership function is shown in the equation below:

$$\mu[x] = \begin{cases} \dfrac{b-x}{b-a}; & a \le x \le b \\ 0; & x \ge b \end{cases} \quad (34)$$

The triangular curve representation consists of two intersecting lines. The shoulder shape curve representation features an area in the middle of a variable, depicted as a triangle. The membership function for the triangular curve representation is as follows:

$$\mu[x] = \begin{cases} 0; & x \le a \; or \; x \ge c \\ \dfrac{x-a}{b-a}; & a \le x \le b \\ \dfrac{b-x}{c-b}; & b \le x \le c \end{cases} \quad (35)$$

The trapezoidal curve representation is essentially similar to a triangle, but with several points that have a membership value of 1.

$$\mu[x] = \begin{cases} 0; & x \le a \; or \; x \ge d \\ \dfrac{x-a}{b-a}; & a \le x \le b \\ 1; & b \le x \le c \\ \dfrac{d-x}{d-c}; & x \ge d \end{cases} \quad (36)$$

The Mamdani method involves four stages to generate output: the formation of fuzzy sets, the application of implication functions, rule composition, and finally, defuzzification (see in Fig. 5). This approach is also utilized in [13], [14].

a) Formation of Fuzzy Sets: Input and output variables are divided into one or more fuzzy sets.

b) Implication Function Application: The Min (minimum) implication function is used, truncating the output of the fuzzy set.

c) Composition of Rules: Unlike monotonous reasoning, when the system consists of multiple rules, the inference is derived from the aggregation and correlation of these rules.

d) Defuzzification: The input for the defuzzification process is a fuzzy set derived from the composition of fuzzy rules. The output produced is a specific number within the fuzzy set domain.

Each membership function consists of five sets with triangular and trapezoidal curves as in [15] using fuzzy Mac Vicar-Whelan rules. The set consists of negative big (NB), negative small (NS), zero (Z), positive small (PS), and positive big (PB). Judging from the membership function applied, 25 if-then rules are formed as in Table 3.

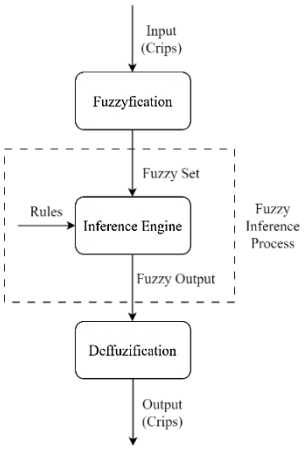

Fig. 5. Fuzzy controller structure

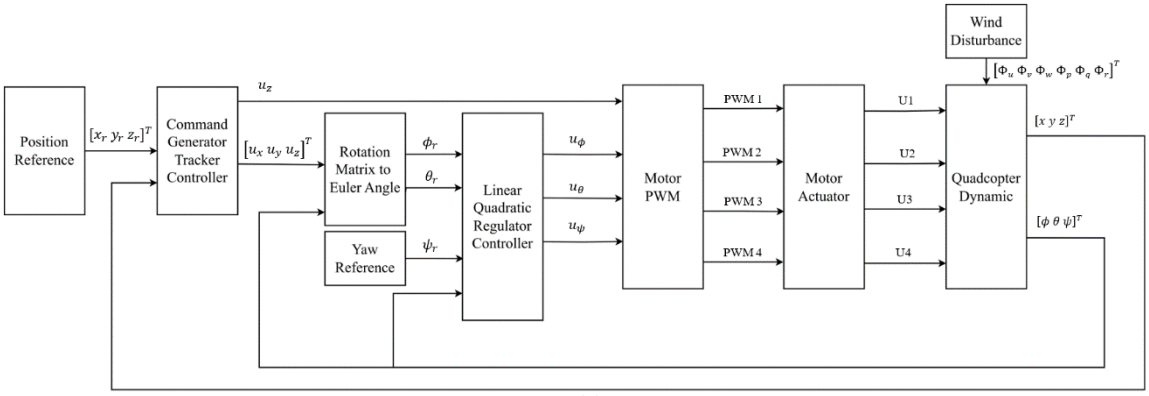

(a)

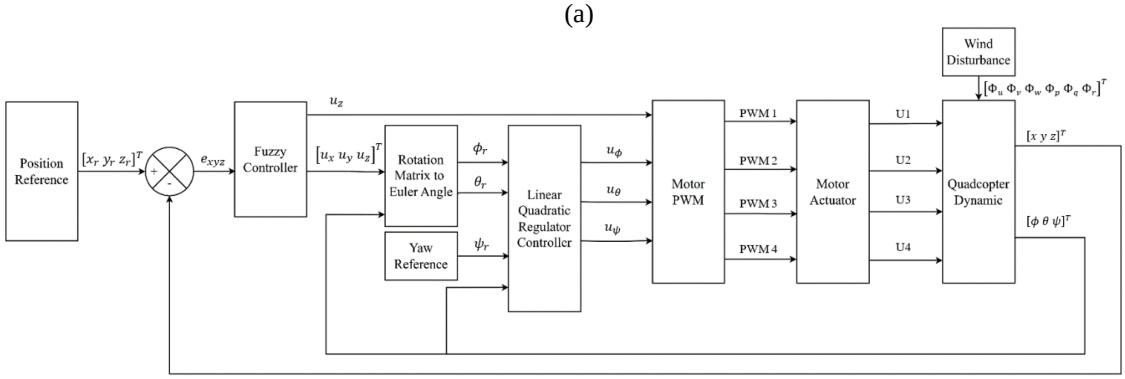

(b)

Fig. 6. Block diagram of the overall quadcopter system using position control (a) CGT controller (b) Fuzzy controller

TABLE 3. FUZZY RULE BASE

e / Δe	**NB**	**NS**	**Z**	**PS**	**PB**
NB	NB	NB	NS	NS	Z
NS	NB	NB	NS	Z	Z
Z	NS	NS	Z	PS	PS
PS	Z	Z	PS	PB	PB
PB	Z	PS	PS	PB	PB

III. RESULTS AND DISCUSSION

In this simulation, a quadcopter will be tested to maintain its mission by carrying a payload when wind turbulence occurs. The payload effect will be directly calculated in the quadcopter dynamics based on (12). The controller applied to the quadcopter is LQR output feedback with Command-Generator Tracker and Fuzzy with LQR output feedback. The arrangement of the quadcopter system with its controller can be seen in Fig. 6. The applied turbulent wind is divided into several strengths such as 0%, 10%, and 50% of the total turbulent wind strength that comes out of the Dryden model wind disturbance block system by Matlab Simulink (see Figure 7 and Figure 8). Then we will compare based on the results of the simulation data obtained to get the best results in dealing with external wind disturbances.

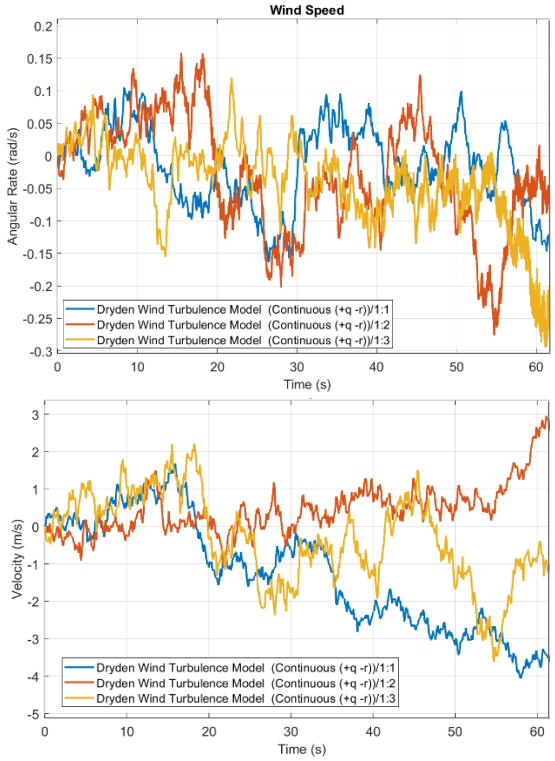

Fig. 7. Wind turbulence speed (angular rate and linear velocity)

A. *Dryden Wind Speed Model*

Turbulent wind flow is random fluctuations that occur continuously and are accompanied by constant winds. Various natural factors can cause turbulent winds based on research [4], [6]. Instances of these factors include wind shifts, air heat exchange, topographic influences, and such. There are two

known turbulence models in [9], the Dryden model and the Von Karman model. In this research, the author uses the Dryden model because the differences in calculating the spectral function and turbulence correlation function of the two models are almost the same. However, there are differences in the slope of the high-frequency band in the spectral function. Therefore, both can be utilized to address the issue under consideration.

Fig. 7 is a graph of the Dryden turbulent wind speed model. The graph is obtained based on the Simulink block of the Dryden wind turbulent model which is available in the MATLAB application. The graph that experiences changes is the same as that illustrated in Fig. 3, where legend number 1 is Φ_u, legend number 2 is Φ_v, legend number 3 is Φ_w, the rising graph is symbolized $-w$, and the falling graph is symbolized $+w$.

B. Simulation with Open-Loop System

The first simulation will be carried out in an open-loop to determine the response of the quadcopter system without gaining feedback. The simulation will be carried out without external wind interference. In Fig. 9, we can see the quadcopter walking upwards or taking off until it reaches the point of infinity. The initial set point z is towards point 1, x is at point 0, and y is at point 0. When the time comes for the quadcopter to hover, the quadcopter cannot do this because there is no feedback on the actual position to calculate the position error.

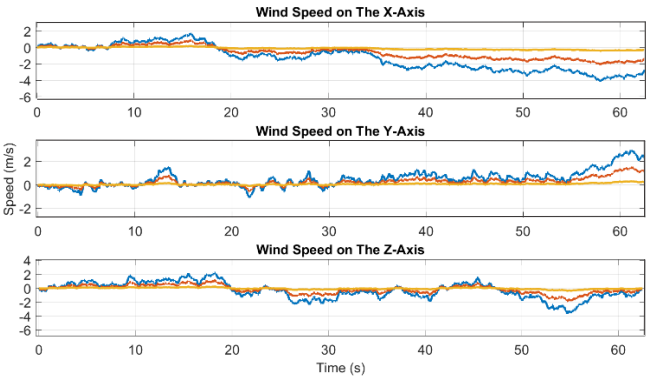

(a)

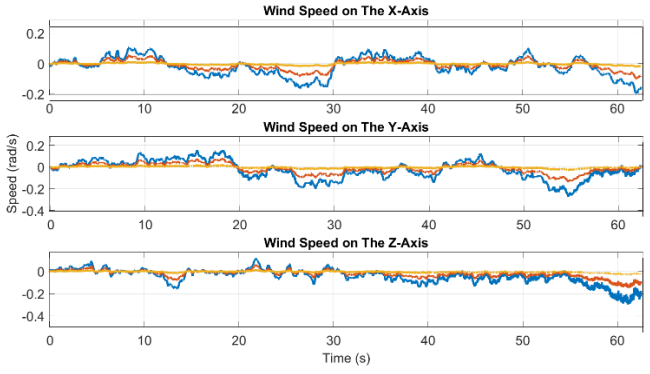

(b)

Fig. 8. The difference in wind speed where the yellow line is 10% speed, the red line is 50% speed, and the blue line is 100% speed or the actual speed of (a) Linear wind speed and (b) Angular wind speed

C. Simulation using LQR with Command-Generator Tracker

The controller applied is a controller from previous researchers without changing the gain weight. This is to find out whether the LQR output feedback with the proposed Command Generator Tracker can overcome wind turbulence if it occurs suddenly when the quadcopter is released in the wild. Turbulent winds will occur at certain points when the quadcopter is carrying out a mission in its reference trajectory.

Wind Turbulence Speed by 0%

The results of a quadcopter simulation using LQR output feedback with Command Generator Tracker without any external wind interference are shown in Fig. 10. The results show that the quadcopter can follow the specified reference trajectory. This means the system can work well if it has a track that resembles a loiter or circle. This can be caused by the characteristics of tracking error with LQR which allows the error at $t = \infty$ to be zero.

Wind Turbulence Speed by 10%

The results from a quadcopter simulation using LQR output feedback with Command Generator Tracker, shown in Fig. 11. This illustrates that the quadcopter has wind interference in certain areas. The applied wind strength is 10% of the total strength. The results show that the quadcopter can still follow the specified reference trajectory. Even when turbulent winds blow, the quadcopter has little shift in its trajectory.

Wind Turbulence Speed by 50%

The results from a quadcopter simulation using LQR output feedback with Command Generator Tracker are detailed in Fig. 12. The results show that the quadcopter has a deviation that is starting to move away even though it can still follow the specified reference trajectory. If wind turbulence occurs continuously, the quadcopter may crash because the wind will blow hard in terrain that is difficult for humans to reach as controllers at the ground control station.

Therefore, a fuzzy controller will be applied to compare quadcopter control in maintaining its mission. This is also used to maintain the stability of the quadcopter when flying in the air to avoid accidents.

D. Simulation using Fuzzy Controller

The fuzzy controller applied in this system will be placed in the quadcopter position control. The selection of membership sets and tuning is done by trial and error to get the best results.

Wind Turbulence Speed by 0%

The results from a quadcopter simulation using fuzzy in conditions without external wind turbulence interference are shown in Fig. 13. The simulation results show that the quadcopter can follow the reference trajectory as in Fig. 10. This shows that the fuzzy controller can work well with the LQR output feedback controller to follow the reference trajectory without any wind interference. So, the next stage is given interference in the form of wind turbulence to test whether the controller can still work well or not.

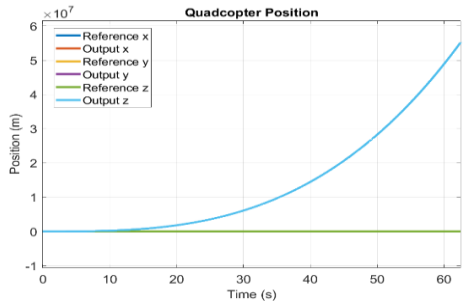

Fig. 9. Open-loop system simulation results

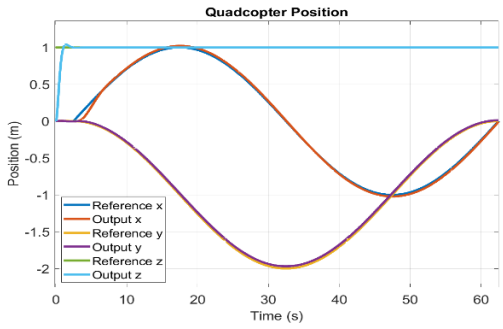

Fig. 10. Simulation results using LQR with Command-Generator Tracker in the absence of wind

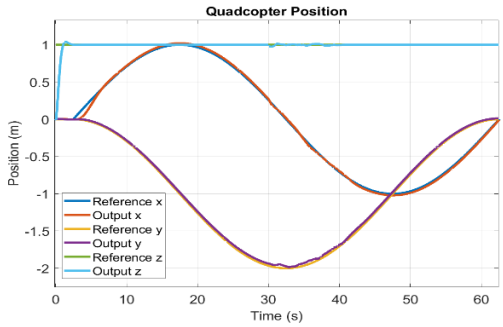

Fig. 11. Simulation results using LQR with Command-Generator Tracker under wind strength conditions of 10%

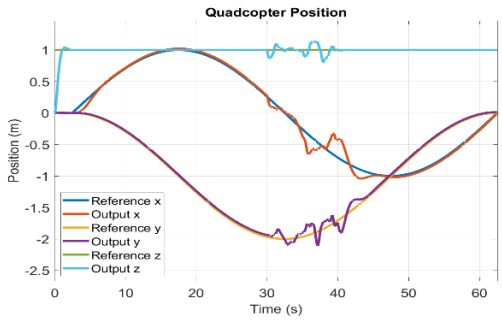

Fig. 12. Simulation results using LQR with Command-Generator Tracker under wind strength conditions of 50%

Wind Turbulence Speed by 10%

The results from a quadcopter simulation using fuzzy, shown in Fig. 14. Thus, the wind disturbance applied to specific areas aligns with the previous simulation using the LQR output feedback with CGT. The simulation results show that the quadcopter can follow the reference trajectory as in Fig. 11. This indicates that the fuzzy and LQR output feedback controller can still control the quadcopter under small-scale wind turbulence disturbances.

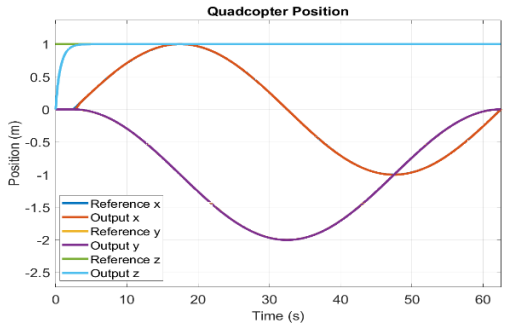

Fig. 13. Simulation results with strengthening the fuzzy controller in conditions without wind

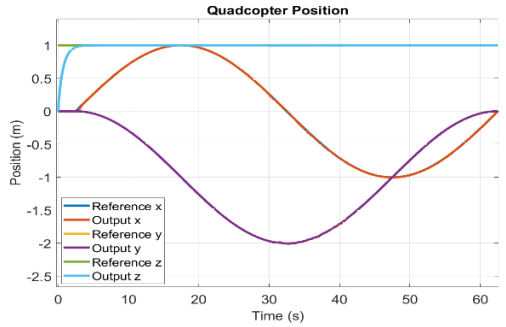

Fig. 14. Simulation results with strengthening the fuzzy controller in wind speed conditions of 10%

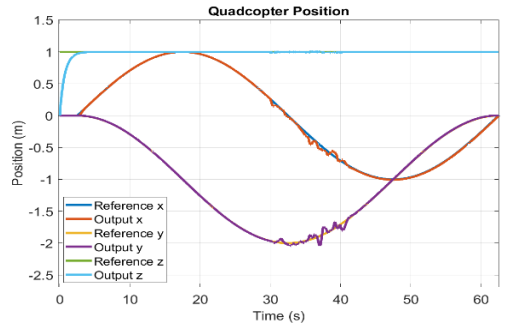

Fig. 15. Simulation results with strengthening the fuzzy controller in wind speed conditions of 50%

Wind Turbulence Speed by 50%

The results from a quadcopter simulation using fuzzy, with a turbulent wind disturbance of 50% are shown in Fig. 15. The simulation results show that the quadcopter can follow the reference trajectory as in Fig. 12. This indicates that a simple fuzzy controller can provide a significant influence when there is quite large wind turbulence disturbance. Apart from that, this is supported by the Linear Quadratic Regulator (LQR) output feedback controller on the attitude control which has an asymptotically stable regulator system so that $e(t)$ approaches zero [12].

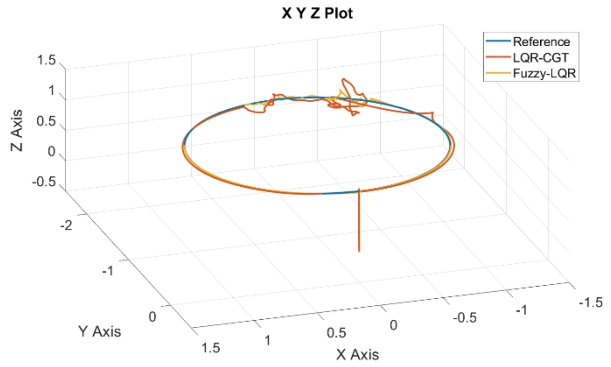

Fig. 16. Simulation results on a 3D trajectory with a wind turbulence speed of 50%

TABLE 4. RSME WHEN QUADCOPTER IN WIND TURBULENCE

RMSE		LQR-CGT	Fuzzy-LQR
50%	*X*	0.0755	0.0183
	Y	0.0516	0.0212
	Z	0.0848	0.0822

Based on the simulation results, quadcopter graphics affected by wind disturbances can be controlled using a fuzzy controller. To prevent the quadcopter deviation from increasing beyond the reference. RMSE comparison can be seen in Table 4. Based on the trajectory, it can be seen in Fig. 16. It can be seen that the quadcopter's movements become aggressive when exposed to wind turbulence. Thus, it is important to control the quadcopter when affected by turbulent external winds.

IV. CONCLUSION

Based on the simulation results of a quadcopter with LQR output feedback control with the Command Generator Tracker, following the reference path can be done well. However, when faced with wind turbulence that was half its original strength, the quadcopter's movement and trajectory deviation began to drift away. Hence, a fuzzy controller is proposed to see the comparison of the two controllers in maintaining the quadcopter's resistance to wind turbulence. The simulation results show that the quadcopter can maintain itself, as seen from the reference trajectory image with the actual trajectory of the quadcopter in the simulation using wind turbulence strength of 50%. If we look at the RMSE values on the x, y and z axes, the LQR-CGT controller each has a value of 0.0755; 0.0516; and 0.0848. Whereas, the Fuzzy-LQR controller each has a value of 0.0183, 0.0212, and 0.0822. Therefore, the fuzzy controller combined with LQR output feedback can support the quadcopter in the midst of wind turbulence.

REFERENCES

[1] T. Agustinah, F. Isdaryani, and M. Nuh, "Tracking control of quadrotor using static output feedback with modified command-generator tracker," *International Review of Automatic Control*, vol. 9, no. 4, pp. 242–251, 2016, doi: 10.15866/ireaco.v9i4.9431.

[2] A. T. Nugraha and T. Agustinah, "Quadcopter Path Following Control Design Using Output Feedback with Command Generator Tracker LOS Based at Square Path," in *Journal of Physics: Conference Series*, Institute of Physics Publishing, Jan. 2018. doi: 10.1088/1742-6596/947/1/012074.

[3] A. Daadi, H. Boulebtinai, S. H. Derrouaoui, and F. Boudjema, "Sliding Mode Controller Based on the Sliding Mode Observer for a QBall 2+ Quadcopter with Experimental Validation," *International Journal of Robotics and Control Systems*, vol. 2, no. 2, pp. 332–356, 2022, doi: 10.31763/ijrcs.v2i2.693.

[4] A. ' Dilah Baharuddin, M. Ariffanan, and M. Basri, "Trajectory Tracking of a Quadcopter UAV using PID Controller," vol. 22, no. 2, pp. 14–21, 2023.

[5] S. I. Azid, K. Kumar, M. Cirrincione, and A. Fagiolini, "Robust motion control of nonlinear quadrotor model with wind disturbance observer," *IEEE Access*, vol. 9, pp. 149164–149175, 2021, doi: 10.1109/ACCESS.2021.3124609.

[6] B. H. Wang, D. B. Wang, Z. A. Ali, B. Ting Ting, and H. Wang, "An overview of various kinds of wind effects on unmanned aerial vehicle," *Measurement and Control (United Kingdom)*, vol. 52, no. 7–8, pp. 731–739, Sep. 2019, doi: 10.1177/0020294019847688.

[7] E. Kuantama *et al.*, "PID and Fuzzy-PID Control Model for Quadcopter Attitude with Disturbance Parameter," 2017.

[8] S. V Viktor, F. I. Valery, Z. A. Yuri, S. O. Igor, and B. A. Denis, "SIMULATION OF WIND EFFECT ON A QUADROTOR FLIGHT," vol. 10, no. 4, 2015, [Online]. Available: www.arpnjournals.com

[9] Team 335, "Wind Control Strategy for Quadcopter," 2020.

[10] Air Force – 11 Team, "FLYING QUALITIES OF PILOTED AIRCRAFT," 2004. [Online]. Available: www.dodssp.daps.mil.

[11] T. M. Ichwanul Hakim and O. Arifianto, "Implementation of Dryden Continuous Turbulence Model into Simulink for LSA-02 Flight Test Simulation," in *Journal of Physics: Conference Series*, Institute of Physics Publishing, May 2018. doi: 10.1088/1742-6596/1005/1/012017.

[12] F. L. Lewis, D. Vrabie, and V. L. Syrmos, "OPTIMAL CONTROL," 2012.

[13] A. Imran, I. Robandi, M. Yusuf Mappeasse, and M. Ruswandi Djalal, "Membership Function Optimization of Fuzzy Logic System Using Cuckoo Search Algorithm for Peak Load Forecasting in Indonesian National Holiday," *Journal of Electrical Technology UMY (JET-UMY)*, vol. 5, no. 2, 2021.

[14] S. Kusumadewi and H. Purnomo, *Aplikasi Logika Fuzzy*. Yogyakarta: Graha Ilmu, 2013.

[15] P. Woś, R. Dindorf, and J. Takosoglu, "FUZZY CONTROLLER TO CONTROL THE ACTIVE AIR SUSPENSION," *The Archives of Automotive Engineering – Archiwum Motoryzacji* , vol. 89, no. 3, 2020.